remote sensing

MDPI

Article

Real-Time Classification of Seagrass Meadows on Flat Bottom with Bathymetric Data Measured by a Narrow Multibeam Sonar System

Masahiro Hamana [1,2,*] and Teruhisa Komatsu [1,2]

[1] Atmosphere and Ocean Research Institute, The University of Tokyo, 5-1-5, Kashiwanoha, Kashiwa 277-8564, Japan; komatsu@aori.u-tokyo.ac.jp

[2] Japan Science and Technology Agency, CREST, 4-1-8 Honcho, Kawaguchi, Saitama 332-0012, Japan

* Correspondence: hamana@aori.u-tokyo.ac.jp; Tel.: +04-7136-6229; Fax: +04-7136-6223

Academic Editors: Nicholas Makris, Xiaofeng Li and Prasad S. Thenkabail
Received: 19 October 2015; Accepted: 18 January 2016; Published: 27 January 2016

Abstract: Seagrass meadows, one of the most important habitats for many marine species, provide essential ecological services. Thus, society must conserve seagrass beds as part of their sustainable development efforts. Conserving these ecosystems requires information on seagrass distribution and relative abundance, and an efficient, accurate monitoring system. Although narrow multibeam sonar systems (NMBSs) are highly effective in resolving seagrass beds, post-processing methods are required to extract key data. The purpose of this study was to develop a simple method capable of detecting seagrass meadows and estimating their relative abundance in real time using an NMBS. Because most seagrass meadows grow on sandy seafloors, we proposed a way of discriminating seagrass meadows from the sand bed. We classify meadows into three categories of relative seagrass abundance using the 95% confidence level of beam depths and the depth range of the beam depth. These are respectively two times the standard deviation of beam depths, and the difference between the shallowest and the deepest depths in a 0.5 × 0.5 m grid cell sampled with several narrow beams. We examined *Zostera caulescens* Miki, but this simple NMBS method of seagrass classification can potentially be used to map seagrass meadows with longer shoots of other species, such as *Posidonia*, as both have gas filled cavities.

Keywords: acoustics; narrow multibeam sonar; real-time classification; seagrass

1. Introduction

Seagrass are submersed marine angiosperms that grow mainly on sandy or muddy substrates in shallow coastal and estuarine waters, forming meadows to provide habitat and shelter for many marine organisms [1–3]. Although seagrass meadows are estimated to cover less than 0.2 percent of the global ocean [4], seagrass supports different trophic levels of marine species [5] and are known to be important in spawning, and larval and juvenile stages of many commercially important fish, mollusks and crustaceans [6,7]. They contribute to the marine environment in several ways, fixing carbon via photosynthesis [8], stabilizing bottom sediments with their root systems, and maintaining coastal water quality and clarity through nutrient uptake [9–12].

Human dependence, well-being and socioeconomic development on marine ecosystems for life have been highlighted in numerous studies [13]. Seagrass provides many goods and services to society, making it one of the most valuable marine ecosystems [14,15]. However, human population growth [16] is placing increasing pressure on coastal ecosystems [17]. Most of the seagrass species of the world are already under threat or diminishing [4,8,18], due to human activities and economic development in coastal zones (e.g., [19,20]). Thus, mapping and monitoring of seagrass meadows

are required to conserve these valuable habitats [21]. Various methods have been used to monitor seagrass meadows, ranging from *in situ* observations to remote sensing techniques. *In situ* observation (e.g., visual census) is laborious and time-consuming [3,22], whereas remote sensing uses less human power and time.

The remote sensing techniques used for seagrass mapping can be divided into two categories, optics-based and acoustics-based [22], depending on the method. The former uses high-resolution satellite imagery (e.g., [23,24]), compact airborne spectrographic imagery (e.g., airborne Portable Remote Imaging Spectrometer (PRISM)) (e.g., [25]), or Light Detection and Ranging (LiDAR) (e.g., [26,27]). The latter uses acoustic backscatter (e.g., echosounders ([28–30]), side-scan sonar ([31–36]), and narrow multibeam sonar (NMBS) using many beams with narrow angle in along-track and across-track directions forming a wide swath range (e.g., [37,38])) to map the seafloor and detect seabed features. Although optical remote sensing is suitable for large-scale mapping, it is not applicable in deep bottom or turbid waters, due to light attenuation in the water column. Additionally, this method is limited by the spatial and radiometric resolution of the satellite images, which may prevent identification of small, patchy, or low-density seagrass [22]. In contrast, acoustic remote sensing can be applied in highly turbid or deeper bottom waters, although it is usually applied in smaller areas due to the cost and time limitations associated with echosounder field surveys [22]. NMBS is one of the most effective acoustic tools for mapping seagrass, because it can survey with a broad swath to create a three-dimensional (3D) image of the seagrass meadow [37].

It is well known that acoustic backscattering information can be used to infer seafloor physical and biological properties (e.g., [39,40]). However, the acoustic scatterings of seagrass and seaweed are poorly understood, compared with rock and sediment [41]. The backscattering strength of seagrass beds is usually higher than that of sandy or muddy bottoms, possibly due to gas bubbles inside the foliage, sheath and shoot stem structure [29,30,40–45].

The study by Komatsu *et al.* [37] succeeded in mapping seagrass beds using bottom topography measured by a NMBS for the first time. They were able to distinguish between echoes from seagrass and echoes from the actual seabed. They removed echoes from the seagrass to create a sea bottom without seagrass and subtract the sea bottom topography without seagrass from the sea bottom topography with seagrass to estimate seagrass distributions. They also estimated biomass coupling quadrat sampling of seagrass with volume and area of seagrass estimated by the NMBS that flowering shoots and vegetative shoots occupied, respectively. In a different study, Komatsu *et al.* [38] mapped *Posidonia oceanica* L. in the Gulf of Gabes, Tunisia facing the Mediterranean Sea. They were able to differentiate the seagrass meadows of *P. oceanica* and sand beds at depths ranging from 20 to 30 m using NMBS backscattering information. These studies required extensive post-processing, and multibeam sonar operation needed to be carried out by highly trained personnel due to the complexities associated with calibration and backscattering processes. In addition, the acquisition data volume by a NMBS is larger than that by echosounder and sidescan sonar processors [46].

Di Maida *et al.* [47] investigated the differentiation of seagrass meadows from sandy beds using bathymetry data obtained with the NMBS. They demonstrated that the NMBS was capable of discriminating between *P. oceanica* meadows and sand substrate via decision-tree post-processing with use of the standard deviation of beam depths or beam depth range within the grids of the bathymetry map. The grids were classified into two categories, based on the presence or absence of high-density seagrass. Recent studies using a NMBS have explored the possibility of discriminating between seagrass and macroalgae, to estimate abundance (dense or sparse) from backscattering measurements [40]. However, their methodology is highly complicated and their results remain inconclusive although discrimination between the presence and absence of meadows was within acceptable limits (78% accuracy in [40]).

The processing and analysis of backscattering strength data from the NMBS is still in the development stages. There is no standard approach for NMBS application [39]. However, bathymetry data processing has advanced to the point of survey area mapping in real time [48]. In this study,

we developed a method to map seagrass meadows and estimate their relative abundance on sand beds by using only bathymetry data which simplify post-process analysis. The proposed system can be used to map seagrass meadows with long shoots growing in the sublittoral zone in real time.

2. Materials and Methods

2.1. Survey Area

The survey area was located off Hadenya in Shizugawa Bay, facing the Pacific Coast of Japan (Figure 1). This was one of the areas most affected by the huge tsunami caused by the East Japan Great Earthquake of 11 March 2011. Tsunamis are known to cause substantial damage to coastal environments and coastal seagrass meadows [49]. Although the seagrass beds in our survey area were seriously affected by the tsunami of 2011 [50,51], the seagrass meadows have recovered to some extent. In the survey area, patches of only one species of seagrass, *Zostera caulescense* Miki were found on a shallow sandy bottom at depths around 6 m prior to the tsunami on 11 March 2011, and have recovered in 2014. On 17 July 2014, an area of 350 × 300 m was surveyed using a NMBS to estimate the area covered with seagrass meadows and relative abundance of seagrass.

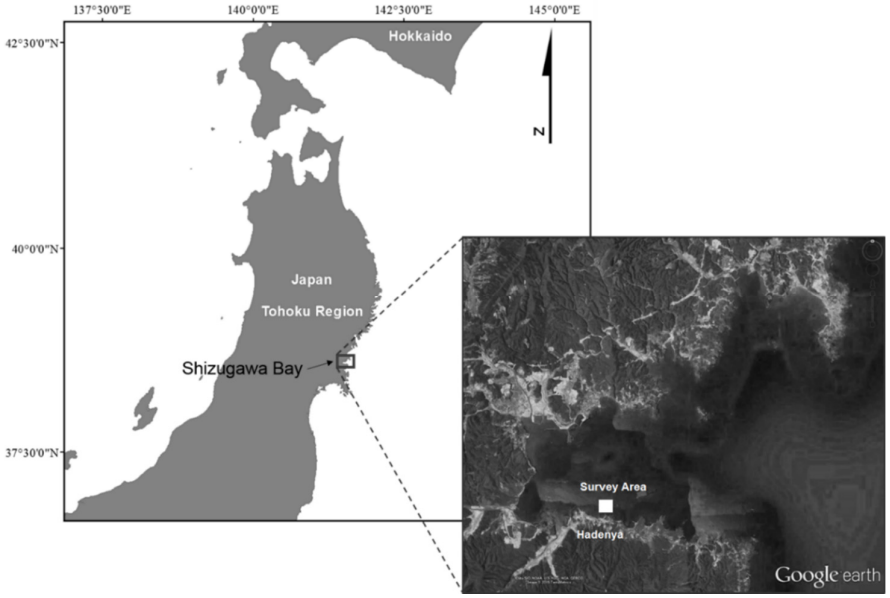

Figure 1. Map showing northern Japan (**left panel**) and Shizugawa Bay (survey area indicated), along with a satellite image from Google Earth (**right lower panel**).

2.2. Data Acquisition

A high-resolution shallow-water NMBS, Sonic 2024 (R2SONIC, Inc., Singapore), was used in the survey. This NMBS collects 256 beam depths for each ping and provides variable swath coverage ranging from 10° to 160°. Operating frequencies can be selected every 10 kHz, ranging from 200 to 400 kHz. The swath coverage and the operating frequency were set to 150° and 380 kHz, respectively, because the frequency of 380 kHz could detect seagrass precisely within the swath angle of 150°. Across- and along- track angles of beam are about 0.6 and 1 degrees width at 380 kHz, respectively. The NMBS used a power of 209 dB, a gain of 14 dB, a pulse duration of 75 μs, a TVG setting of 20 Log$R$ (R = slant range), an absorption coefficient of 0 dB· m^{-1}, and a ping rate of 10 Hz. Since the absorption coefficient is highly influenced by salinity and water temperature profiles, we measured them before and after the survey. If the absorption coefficient is set before the survey, it is complicated to change it with the corrected coefficient in post-processing. The absorption coefficient was set to 0 dB· m^{-1} for convenience of post-processing.

Position and motion of the NMBS transducer (roll, pitch, heave, and heading) were measured by the inertial navigation system "POS/MV" (Applanix Corp., Richmond Hill, ON, Canada). The positioning accuracy of POS/MV varied from 0.5 to 2 m (Differential GPS mode) [52]. Sonic 2024 and POS/MV were installed on a small fishing boat (about 1 gross ton) (Figure 2). Both Sonic 2024 and POS/MV data were collected and analyzed using the multibeam processing software QINSy (Quality Integrated Navigation System, QPS Co., Zeist, The Netherlands). The dynamic correction (boat roll, pitch and heave) to NMBS data was applied in real time in the field.

The survey was conducted in day time on 17 July 2014 in the seagrass meadow off Hadenya in Shizugawa Bay. The seagrass meadow was distributed over an area estimated at approximately 300 m in length and 100 m in width in the survey area of about 350 × 250 m. We established ten observation points of Stns. 1 to 10 along a transversal line in the middle of the seagrass patch, to collect NMBS and ground truth data (Figure 3). At these stations, NMBS data with GPS (POS/MV system) and underwater-cased video camera (GoPro HERO 3, GoPro Inc., San Mateo, CA, USA) data were recorded simultaneously. The bottom substrate was recorded by the NMBS and the video camera that was lowered from the boat. A buoy was cast for scuba diving investigation; the buoy position of each station was extracted from POS/MV system data. Scuba divers also took underwater photos on the sea bottom at each station. After collecting the data from the stations, the entire meadow was surveyed using a total of 16 parallel transects (length: 350 m) at 15 m intervals (Figure 3). The swath coverage of the NMBS is around 44 m wide at a bottom depth of 6 m, so the swath coverage of transects was overlapped at 70% including overlaps of both sides of neighboring transects. A towed video survey was done after the transect survey of NMBS (Figure 3). The position data during a video recording were collected by POS/MV system.

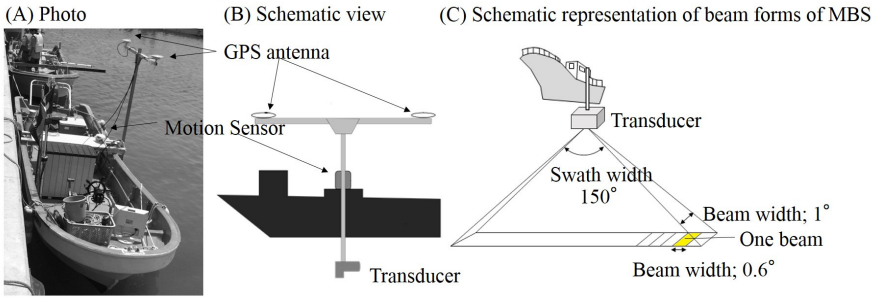

Figure 2. Narrow multibeam sonar (NMBS), global positioning system (GPS), and motion sensor mounted on the small boat: (**A**) photo of fishing boat equipped with the NMBS; (**B**) schematic view of the NMBS installed on the boat and (**C**) beam forms of NMBS.

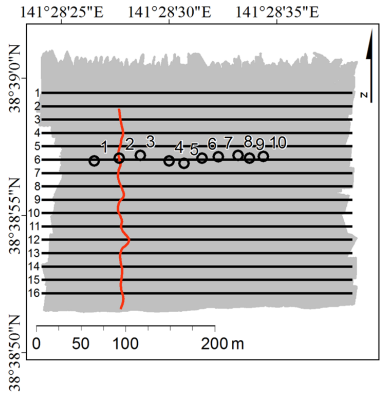

Figure 3. Planned survey transects (solid lines) and stations (open circles) indicated by a number (1–16) to the left of the line and station number (1–10) along the transect of Line 6, respectively. The red line is a towed video survey line. The grey area is the area surveyed with the NMBS.

2.3. Data Analysis

Video shots and underwater photos of the sea bottom at Stns. 1 to 10 were taken by an underwater-cased video camera lowered from the boat as a drop camera and by divers on the sea bottom, respectively, for evaluating relative abundance of seagrass at the ten stations. To verify whether seagrass produced detectable echoes, water column acoustic images (WCIs) produced with the NMBS were simultaneously recorded with the software QINSy during the ground survey at Stns. 1 to 10. WCIs were visually compared with the video shots synchronized with WCIs by their recording time. Underwater photos of the sea bottom were used for qualitatively assessing relative abundance of seagrass at the ten stations, consulting references on seagrass coverage estimation guide [40,53]. According to the images and videos, relative abundance of seagrass at each station was classified into three categories: Category A (dense seagrass), Category B (sparse seagrass) and Category C (little to no seagrass).

Acoustic data obtained along the 16 transects were processed with a hydrographic survey software validation tool to remove false depths deeper than the actual seafloor depth, some of which are caused by multiple echoes (Figure 4). Bathymetry maps were created at a grid size of 0.5 × 0.5 m using processed data. We calculated depth range and 95% confidence level (95% CL) of beam depths within each grid cell. Depth range is defined as the distance between the shallowest and the deepest beam depths within a grid cell. Because *Zostera* seagrass shoots and leaves reflect beams from the NMBS, depth range is used as a proxy for difference between seagrass height and bottom [47] (Figure 4). When *Zostera* seagrass grows luxuriantly, seagrass becomes high. Then, we hypothesize that relative abundance of seagrass depends on shoot heights expressed as beam depth range between the top of seagrass and the sand bed within a grid cell of a surveyed area.

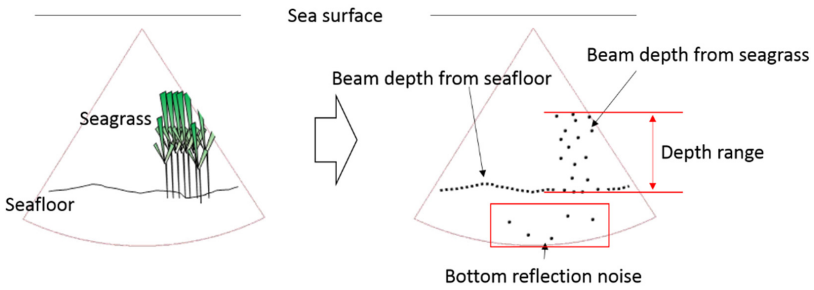

Figure 4. Schematic view of WCI data on seagrass and sand bed collected with a NMBS (**left panel**) and beam depths reflected from the seagrass and the sea bottom including bottom reflection noise (**right panel**).

The 95% CL is a parameter used for data quality evaluation obtained with the software [54,55]. The International Hydrographic Organization (IHO) Standards for Hydrographic Survey [56] define the confidence level as the probability that the true value of a measurement will lie within the specified uncertainty from the measured value. One-dimensional (1D, depth) 95% confidence level is calculated by assuming a normal distribution corresponding to 1.96 times of the standard deviation [56]. If the sea bottom is flat, 95% CL becomes small due to low standard deviation of beam depths reflected by the flat sea bottom. On the other hand, it becomes greater when the sea bottom is rough. Then, we hypothesize that the 95% CL depends on spatial complexity within a grid cell produced by abundance of seagrass growing on the sand bed.

Depth range and 95% CL data of a grid of 0.5 × 0.5 m in the survey area with a grid position were imported to ArcGIS (ESRI, Inc., Redlands, CA, USA). To test the hypotheses mentioned above, we compared the depth range and 95% CL with relative abundance of seagrass estimated from underwater video and camera images at the ten stations. Values of depth range and 95% CL within a radius of 1 m at each station were created with buffer analysis of ArcGIS. Those at all stations were classified and grouped by relative abundance of seagrass judged from the underwater images.

Threshold values of depth range and 95% CL among categories of relative abundances of seagrass were obtained based on grouped data of depth range and 95% CL by categories of relative abundance.

To assess the accuracy of seagrass map created by NMBS data, the towed video shots and the category of relative abundance of seagrass map were compared. The towed video shots were extracted at 30 points among the survey line at random. Each towed video shots were categorized into three category in the same way as video shots at Stns. 1 to 10. The most frequent category of seagrass abundance in each grid within 1 m radius at each points of towed video shots were extracted by buffer analysis of ArcGIS. The accuracy of seagrass map was assessed to compare the most frequent category of seagrass abundance in each of the thirty points and the seagrass abundance estimated with the towed video shots at each point.

3. Results

3.1. Comparison of Water Column Acoustic Images (WCIs) with the Underwater Images

Figure 5 shows two examples of a comparison of the WCIs with the video shots at Stns. 5 and 10. The video shots showed seagrass abundantly growing on the sand bed at Stn. 5 but not at Stn. 10. The WCIs showed reflection echoes from above-ground parts of seagrass and the sand bed at Stn. 5 but only those from the sand bed at Stn. 10. The beam depths data obtained from the NMBS could draw above-ground parts of seagrass with the sand bed at Stn. 5 and the sand bed at Stn. 10 corresponding to the WCIs and video shots (Figure 5).

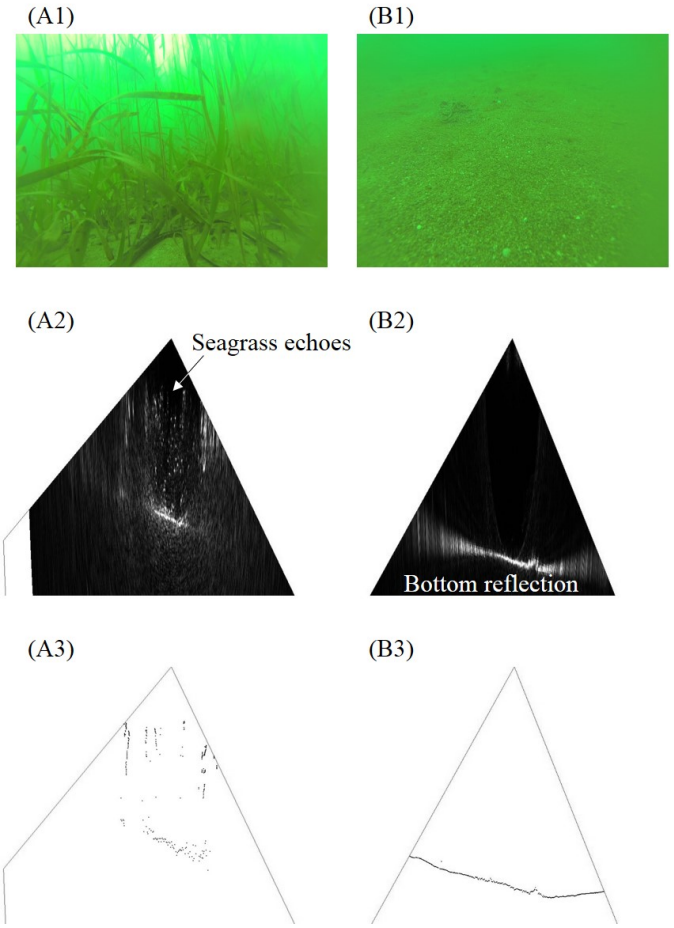

Figure 5. Underwater-cased camera video shots (**A1,B1**), water column acoustic images (**A2,B2**); and beam depth distributions represented with dots (**A3,B3**); (**A,B**) correspond to Stn. 5 with dense seagrass on the sand bed and Stn. 10 with only sand bed, respectively.

3.2. Classification of Stations into Three Categories of Seagrass Relative Abundance

Stations were visually classified into three categories of relative abundance of seagrass based on the underwater photos taken by the divers. Figure 6 shows an example of three different categories of relative abundance: dense, sparse and little or no seagrass. Categories A, B and C were assigned to Stns. 2–5 (dense seagrass), Stns. 1, 6 and 8 (sparse seagrass) and Stns. 7, 9 and 10 (little to no seagrass), respectively (Table 1).

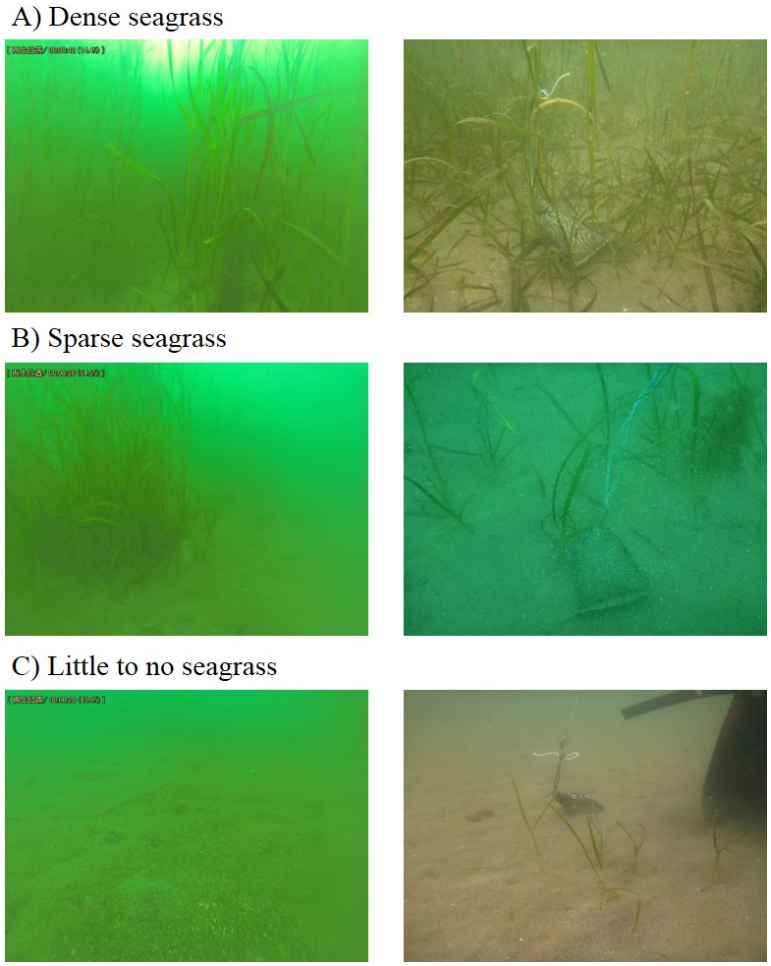

Figure 6. Examples of underwater images consisting of underwater video shots (**left column**) and underwater photo taken by divers (**right column**) belonging to three categories of relative abundance of seagrass: (**A**) dense seagrass at Stn. 4; (**B**) sparse seagrass at Stn. 8 and (**C**) little to no seagrass at Stn. 9.

Table 1. Three categories of relative abundance of seagrass from A to C and their mean values and standard deviation of 95% confidence level (CL) and depth range within 1-m radius from the centre of each station.

Underwater Photo		Acoustic Data (Beam Depth)				
Categories	Stns.	95% Confidence Level		Depth Range (m)		Mean Bottom Depth (m)
		Mean	S.D.	Mean	S.D.	
A	2, 3, 4, 5	1.51	0.22	2.14	0.43	5.74
B	1, 6, 8	0.59	0.14	0.95	0.28	5.77
C	7, 9, 10	0.11	0.12	0.16	0.16	6.02

3.3. 95% CL and Depth Range and Relative Abundance of Seagrass

Mean values of 95% CL and depth range at each category of relative abundance of seagrass were presented in Figure 7. For the 95% CL, the mean values were 1.51, 0.59, and 0.11, for grades A to C, respectively. For the depth range, grades from A to C had values of 2.14, 0.95 and 0.16 respectively.

Both the 95% CL and the depth range had a positive relation with relative abundance of seagrass. As the relative abundance of seagrass became higher, the mean values of both parameters increased. In order to create a relative abundance of seagrass, the middle value of 95% CL and depth range between each grade were used as threshold values for each category. Categories of seagrass were defined as: dense, sparse, or little to no seagrass (Figure 7).

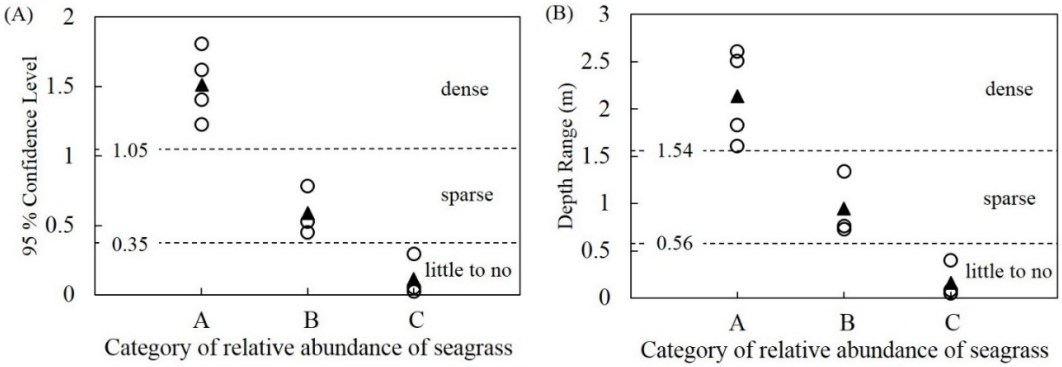

Figure 7. Relationship between (**A**) 95% CL and (**B**) depth range with the relative abundance of seagrass. Open circles and closed triangles indicate mean values of stations classified into each category and category means, respectively. The dashed line shows median value of each category used for the threshold between categories. The threshold values are indicated on the left side of the plot.

3.4. Distribution of Seagrass Meadows

The sea bottom gently inclined north-westwards and a very shallow bottom was distributed along the northeast end (Figure 8a). The high resolution bathymetry map showed that the seagrass meadows were distributed as a turf pattern in an area with bottom depths of around 6 m from the west end to centre area along the transversal direction in the middle latitude part of the map (Figure 8a). Categories of relative abundance of seagrass were mapped by categorizing mean values of depth range and 95% CL within a grid (Figure 8B,C). The area as the turf pattern in the high resolution bathymetry map overlapped with the areas with green and yellow colours of 95% CL and depth range. In the maps of relative abundance of seagrass (Figure 8B,C), categories of sparse seagrasses in the north region, especially northeast corner, where no seagrass was distributed in the high-resolution bathymetry map, were present in the maps of categories of 95% CL and depth range.

The numbers of grid cells for categories of relative abundance of dense and sparse seagrasses based on 95% CL were 49,657 and 17,656 grids equivalent to areas of 12,414.25 m^2 and 4414 m^2 respectively. Those for categories of relative abundance of dense and sparse seagrasses based on depth range were 51,879 and 14,180 grids equivalent to 12,969.75 m^2 and 3545 m^2, respectively. An area with categories of relative abundance of seagrass, excluding the category of little to no seagrass was 16,828.25 m^2 by the former and 16,514.75 m^2 by the latter. The difference of total seagrass area, excluding the category of little to no seagrass between 95% CL and depth range was 313.5 m^2.

Table 2 shows error matrix of seagrass map of 95% CL and depth range. Overall accuracy of depth range (0.83) was slightly higher than of 95% CL (0.80).

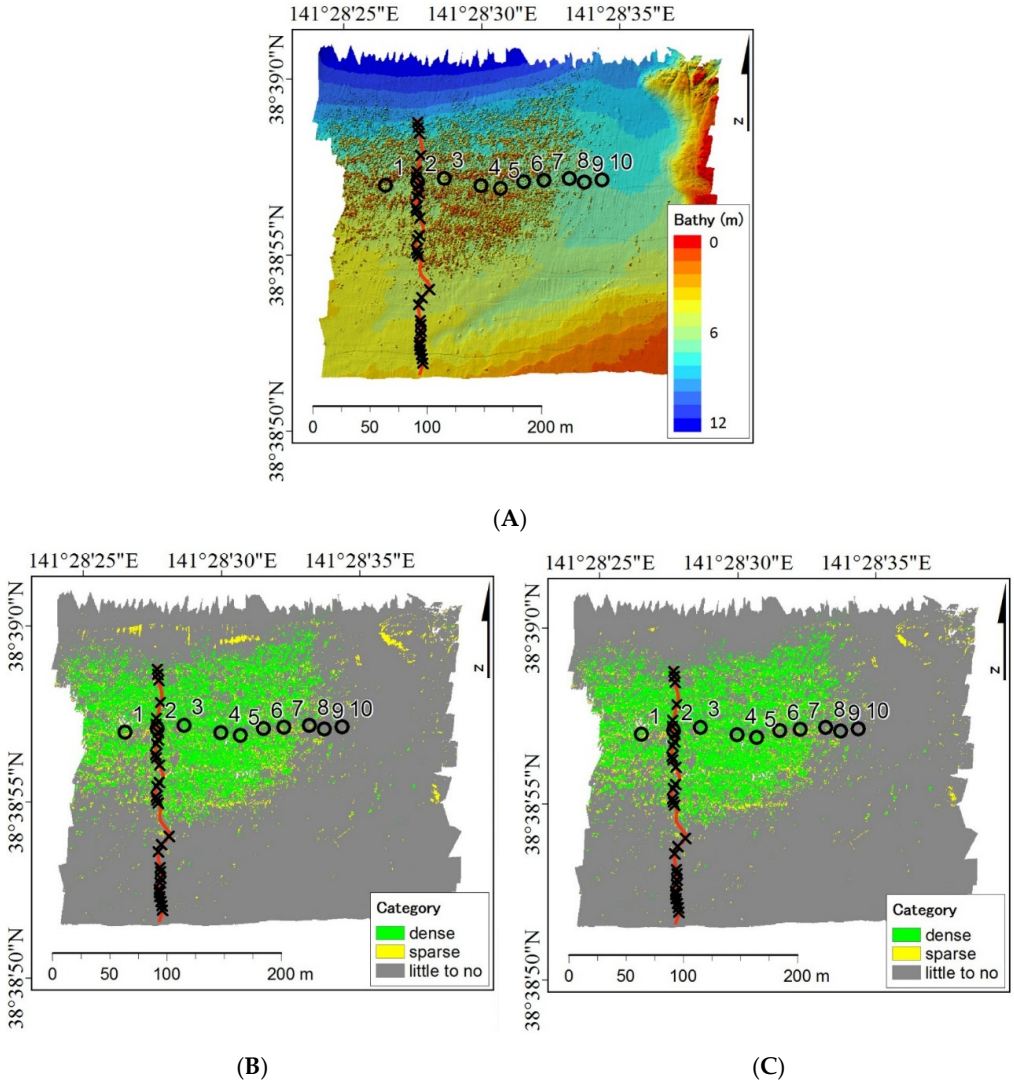

Figure 8. Maps of high-resolution bathymetry (**A**) and relative abundance of seagrass classified with 95% confidence level (**B**) and depth range (**C**). Green, yellow, and grey represent categories of dense, sparse and little to no seagrasses, respectively. Opened circles show Stns. 1–10. The red line shows a towed video survey line. The cross mark presents 30 points extracted among towed video survey line at random.

Table 2. Error matrix for seagrass map: (A) 95% confidence level and (B) depth range.

(A) 95% Confidence Level		Reference Data			User Accuracy
		Dense	Sparse	No	
Classified	Dense	6	1	0	0.86
	Sparse	1	1	0	0.50
	Little to No	4	0	17	0.81
Producer accuracy		0.55	0.50	1.00	Overall accuracy 0.80
(B) Depth Range		**Reference Data**			**User Accuracy**
		Dense	**Sparse**	**No**	
Classified	Dense	8	1	1	0.80
	Sparse	1	1	0	0.50
	Little to No	2	0	16	0.89
Producer accuracy		0.73	0.50	0.94	Overall accuracy 0.83

4. Discussion

Seagrass echoes are recorded as beam depths and are observed as a turf pattern consisting of many small peaks in the high-resolution bathymetry map. This area also corresponds to the areas with relative abundance of seagrass from low to high seagrass categories classified with depth range and 95% CL. Therefore, it is possible to map seagrass beds with both depth range and 95% CL. Distributions and areas of three categories based on depth range were similar to those based on 95% CL. In flat bottom areas, both the 95% CL and the depth range showed good correspondence with the relative abundance of seagrass. Since Di Maida *et al.* [47] suggested that the depth range is highly influenced by the seagrass shoot length of *Posidonia oceanica* L., it is natural that depth range reflects seagrass distributions. This study shows that 95% CL is also influenced by shoot length and density within a grid. Thus, depth range and 95% CL are very practical for mapping seagrass distributions with categories of relative abundance of seagrass.

During the surveys, *in situ* acquisition of data with some hydroacoustic survey software can display maps of 95% CL or depth range of a grid surveyed in real time with different colours depending on designated values for 95% CL or depth range in a grid cell set before the *in situ* survey. This potentially enables visualization and mapping of relative abundance of seagrass in real time during the field survey.

In the northeast corner with shallower rough seafloor, categories of relative abundance of dense and sparse seagrass classified with depth range and 95% CL were found. The rugged bottom topography influences the depth range and the 95% CL. Therefore, these categories also appeared in the northwest corner. However, it is obvious that rugged bottom can be distinguished from seagrass meadow using the bottom topography. In the bathymetry map, seagrass meadow appears as many small peaks on the flat sand bed, while rough seafloor or rugged bottom do not have these peaks. Thus, it is easy to distinguish seagrass meadows from rugged bottom by using the bathymetry map.

Although the above-mentioned problem exists, mapping categories of relative abundance of seagrass using the 95% CL or depth range has several advantages over post-processing methods (e.g., [37]). The first advantage is that seagrass relative abundance can be mapped in real time using some hydrographic survey software when collecting field data. The second advantage is that the proposed method creates a high-resolution seagrass map such as 0.5 × 0.5 m in real time.

Several studies have approached the mapping of seagrass beds using acoustic sonars, but mapping of its abundance is an ongoing process. Tecchiato *et al.* [40] investigated the discrimination and estimation of the relative abundance of seagrass and seaweed in Western Australia using NMBS backscattering data and reported that the acoustic response from seagrass, macroalgae, and a low-density mix of the two were too similar for discrimination based on acoustic backscattering properties. They used the angle cube method developed by Parnum [42] to analyze NMBS backscattering strengths. Although the angle cube method is a powerful method for visualising seafloor backscatter strength data, processing of the data can be complicated and the grid cell size is nearly 2 × 2 m due to spatial interpolation [40–42,57]. In general, seagrass meadows have a complex structure including small patches that change from higher density areas to lower density ones over short distances. Sometimes, seagrass meadows have uncolonized areas inside the patch such as gaps. In this situation, smaller grid cell sizes are more likely to be realistic and to represent the seagrass distribution. Using the 0.5 × 0.5 m grid cell size in this study, we were able to reproduce low-density seagrass patches and gaps of uncolonized areas inside the meadow (Figure 8). Grid cells sizes of less than or equal to 0.5 × 0.5 m are desirable for seagrass mapping studies.

5. Conclusions

The most important advantage of the proposed technique is that the relative abundance of seagrass on the flat sand bottom can be estimated in real time using both the 95% CL and the depth range. Most of the hydrographic survey software for collecting sea bottom data during surveys can display *in situ* 95% CL, and standard deviation of depth range or depth range of grid cells with different colors

using personalized threshold values. Thus, it is possible to visually obtain an overview of the relative abundance of seagrass distribution in real time. Additionally, the simplicity of both the collection method and post-processing allow for continued monitoring of specific areas with less sampling effort and shorter processing times.

Acknowledgments: We are grateful to Satoshi Watanabe, Minoru Suzuki and Kazufumi Sato of the Shizugawa Fishermen Cooperative and the Shizugawa Fishermen Cooperative for their kind help and permission with our field study. We also wish to thank Fumitaka Maeda and Yusuke Sato of Toyo Corporation for their technical assistance, and Shuji Sasa, Shingo Sakamoto, Sara Gonzalvo Maro, and other members of the Laboratory of Behavior, Ecology and Observations Systems of the Atmosphere and Ocean Research Institute, the University of Tokyo for their help, constructive discussions, and encouragement during this study. This study was supported by research grants from the Japan Science and Technology Agency (JST/CREST), the Environment Research and Technology Development Fund (S13) of the Ministry of the Environment in Japan and Tohoku Ecosystem-Associated Marine Sciences funded by the Ministry of Education, Culture, Sports, Science and Technology in Japan.

Author Contributions: Both authors collaborated in the design of the experiment and data collection. Masahiro Hamana performed the data analysis and writing of the manuscript, with comments and support from Teruhisa Komatsu.

Conflicts of Interest: The design of this experiment and preliminary results were displayed during a poster presentation on the ICES SomeAcoustic conference in Nantes, France in May of 2015.

References

1. Boudouresque, C.F. Les Herbiers à *Posidonia oceanica*. In *Préservation et Conservation des Herbiers à Posidonia Oceanica*; Boudouresque, C.-F., Bernard, G., Bonhomme, P., Charbonnel, E., Diviacco, G., Meinesz, A., Pergent, G., Pergent-Martini, C., Ruitton, S., Tunesi, L.L., Eds.; Ramoge Publication: Monaco, 2006; pp. 10–24.
2. Díaz-Almela, E.; Duarte, C.M. *Management of Natura 2000 habitats. 1120* Posidonia beds (Posidonion oceanica)*; European Commission: Brussels, Belgium, 2008.
3. Buchet, V. Impact Assessment of Invasive Flora Species in Posidonia Oceanica Meadows on Fish Assemblage: an Influence on Local Fisheries?: The Case Study of Lipsi Island, Greece. Master's Thesis, University of Akureyri, Akureyri, Island, 31 March 2015.
4. Duarte, C.M. The future of seagrass meadows. *Environ. Conserv.* **2002**, *29*, 192–206.
5. Orth, R. J.; Carruthers, T.J.B.; Dennison, W.C.; Duarte, C.M.; Fourqurean, J.W.; Heck, K.L., Jr.; Randall, A.H.; Kendrick, G.A.; Kenworthy, W.J.; Olyarnik, S.; *et al*. A global crisis for seagrass ecosystems. *Bioscience* **2006**, *56*, 978–996. [CrossRef]
6. Jackson, E.L.; Rowden, A.A.; Attrill, M.J.; Bossey, S.; Jones, M. The importance of seagrass beds as a habitat for fishery species. *Oceanogr. Mar. Biol.* **2001**, *39*, 269–304.
7. Bertelli, C.M.; Unsworsth, R.K.F. Protecting the hand that feeds us: Seagrass (Zostera marina) serves as commercial juvenile fish habitat. *Mar. Pollut. Bull.* **2014**, *83*, 425–429. [CrossRef] [PubMed]
8. Short, F.T.; Beth, P.; Livingstone, S.R.; Carpenter, K.E.; Salomão, B.; Bujang, J.S.; Calumpong, H.P.; Carruthers, T.J.B.; Coles, R.G.; Dennison, W.C.; *et al*. Extinction risk assessment of the world's seagrass species. *Biol. Conserv.* **2011**, *144*, 1961–1971. [CrossRef]
9. Ward, L.G.; Kemp, W.M.; Boyton, W.R. The influence of waves and seagrass communities on suspended particulates in an estuarine embayment. *Mar. Geol.* **1984**, *59*, 85–103. [CrossRef]
10. Jeudy de Grissac, A.; Boudouresque, C.-F. Rôle des herbiers de Phanérogames marines dans les mouvements des sédiments côtiers: Les herbiers à *Posidonia oceanica*. In *Acte du Colloque Pluridisciplinaire Franco-Japonais d'Océanographie Fiscicule 1*; Ceccaldi, H.J., Champalbert, G., Eds.; Société Franco-japonaise d'Océanographie, Marseille: Marseille, France, 1985; pp. 143–151.
11. Komatsu, T. Influence of a *Zostera* bed on the spatial distribution of water flow over a broad geographical area. In Proceedings of an International Workshop Conference on Seagrass Biology, Nedlands, Australia, 25–29 January 1996; pp. 111–116.
12. Komatsu, T.; Yamano, H. Influence of seagrass vegetation on bottom topography and sediment distribution on a small spatial scale in the Dravuni Island Lagoon, Fiji. *Biol. Mar. Mediterr.* **2000**, *7*, 243–246.

13. Cullen-Unsworth, L.C.; Mtwana Nordlund, L.; Paddock, J.; Baker, S.; McKenzie, L.J.; Unsworth, R.K.F. Seagrass meadows globally as a coupled social-ecological system: Implications for human well-being. *Mar. Pollut. Bull.* **2014**, *83*, 387–397. [CrossRef] [PubMed]
14. Costanza, R.D.; Arge, D.; de Groot, R.; Farber, S.; Grasso, M.; Hannon, B.; Limburg, K.; Naeem, S.; O'Neill, R.V.; Paruelo, J.; *et al*. The value of the world's ecosystem services and natural capital. *Nature* **1997**, *387*, 253–260. [CrossRef]
15. Vassallo, P.; Paoli, C.; Rovere, A.; Montefalcone, M.; Morri, C.; Bianchi, C.N. The value of the seagrass *Posidonia oceanica*: A natural capital assessment. *Mar. Pollut. Bull.* **2013**, *75*, 157–167. [CrossRef] [PubMed]
16. Meyer, W.B.; Turner, B.L. Human population growth and global land-use/cover change. *Ann. Rev. Ecol. Syst.* **1992**, *23*, 39–61. [CrossRef]
17. World Bank. *World Development Report 2003: Sustainable Development in a Dynamic World—Transforming Institutions, Growth, and Quality of Life*; World Bank: New York, NY, USA, 2003.
18. Tunesi, L.; Boudouresque, C.-F. Les Causes de la Régression Des Herbiers à *Posidonia oceanica*. In *Préservation et Conservation Des Herbiers à Posidonia Oceanica*; Boudouresque, C.-F., Bernard, G., Bonhomme, P., Charbonnel, E., Diviacco, G., Meinesz, A., Pergent, G., Pergent-Martini, C., Ruitton, S., Tunesi, L., Eds.; Ramoge Publication: Monaco, 2006; pp. 32–47.
19. Komatsu, T. Long-term changes in the *Zostera* bed area in the Seto Inland Sea (Japan), especially along the coast of the Okayama Prefecture. *Oceanol. Acta* **1997**, *20*, 209–216.
20. Komatsu, T.; Sagawa, T.; Sawayama, S.; Tanoue, H.; Mohri, A.; Sakanishi, Y. Mapping Is a Key for Sustainable Development of Coastal Waters: Examples of Seagrass Beds and Aquaculture Facilities in Japan with Use of ALOS Images. In *Sustainable Development*; Ghenai, C., Ed.; Tech Publishing Co.: Rijeka, Croatia, 2012; pp. 145–160.
21. Kirkman, H. Seagrass distribution and mapping. Seagrass research methods. *Monogr. Oceanogr. Methodol.* **1990**, *9*, 19–25.
22. Komatsu, T.; Mikami, A.; Sultana, S.; Ishida, K.; Hiraishi, T.; Tatsukawa, K. Hydro-acoustic methods as a practical tool for cartography of seagrass beds. *Otsuchi Mar. Sci.* **2003**, *28*, 72–79.
23. Hashim, M.; Yahya, N.N.; Ahmad, S.; Komatsu, T.; Misbari, S.; Reba, M.N. Determination of seagrass biomass at Merambong Shoal in Straits of Johor using satellite remote sensing technique. *Malay. Nat. J.* **2014**, *66*, 20–37.
24. Sagawa, T.; Boisnier, E.; Komatsu, T.; Mustapha, K.B.; Hattour, A.; Kosaka, N.; Miyazaki, S. Using bottom surface reflectance to map coastal marine areas: A new application method for Lyzenga's model. *Int. J. Remote Sens.* **2010**, *31*, 3051–3064. [CrossRef]
25. Phinn, S.; Roelfsema, C.; Dekker, A.; Brando, V.; Anstee, J. Mapping seagrass species, cover and biomass in shallow waters: An assessment of satellite multispectral and airborne hyper-spectral imaging systems in Moreton Bay (Australia). *Remote Sens. Environ.* **2008**, *112*, 3413–3425. [CrossRef]
26. Kotchenova, S.Y.; Song, X.; Shabanov, N.V.; Potter, C.S.; Knyazikhin, Y.; Myeni, R.B. Lidar remote sensing for modeling gross primary production of deciduous forests. *Remote Sens. Environ.* **2004**, *92*, 158–172. [CrossRef]
27. Maltamo, M.; Eerikainen, K.; Pitkainen, J.; Hyppa, J.; Vemas, M. Estimation of timber volume and stem density based on scanner laser altimetry and expected size distribution functions. *Remote Sens. Environ.* **2004**, *90*, 319–330. [CrossRef]
28. Hamilton, L.J. Real-time echosounder based acoustic seabed segmentation with two first echo parameters. *Methods Oceanogr.* **2014**, *11*, 13–28. [CrossRef]
29. Komatsu, T.; Tatsukawa, K. Mapping of *Zostera marina* L. beds in Ajino Bay, Seto Inland Sea, Japan, by using echosounder and global positioning systems. *J. Rech. Oceanogr.* **1998**, *23*, 39–46.
30. Sabol, B.M.; Melton, R.E.; Chamberlain, R.; Doering, P.; Haunert, K. Evaluation of a digital echo sounder system for detection of submersed aquatic vegetation. *Estuaries* **2002**, *25*, 133–141. [CrossRef]
31. Newton, R.S.; Stefanon, A. Application of side scan sonar in marine biology. *Mar. Biol.* **1975**, *31*, 287–291. [CrossRef]
32. Meinesz, A.; Cuvelier, M.; Laurent, R. Méthode récentes de cartographie et de surveillance des herviers de Phanérogames marines. *Vie Milieu* **1981**, *31*, 27–34.
33. Lefèvre, J.R.; Meinesz, A.; Gloux, B. *Premières Données sur la Comparaison de Trois Méthôdes de Cartographie des Biocénoses Marines*; Commission Internationale pour L'Exploration Scientifique de la Mer Méditerranée (CIESM): Monaco, 1984.

34. Gloux, B. Méthode Acoustiques et Informatiques Appliquées à la Cartographie Rapide et Détaillée Des Herbiers. In *International Workshop on Posidonia oceanica Beds*; Boudouresque, C.-F., Jeudy de Grissac, A., Olivier, J., Eds.; GIS Posidonie Press: Marseille, France, 1984; pp. 45–48.
35. Ramos, M.A.; Ramos-Espla, A. Utilization of acoustic methods in the cartography of the *Posidonia oceanica* bed in the bay of Alicante (SE, Spain). *Pos. Newslett.* **1989**, *2*, 17–19.
36. Pasqualini, V.; Pergent-Martini, C.; Clabaut, P.; Pergent, G. Mapping of *Posidonia oceanica* using aerial photographs and side scan sonar: Application off Island of Corsica (France). *Estuar. Coast. Shelf Sci.* **1998**, *47*, 359–367. [CrossRef]
37. Komatsu, T.; Igarashi, C.; Tatsukawa, K.; Matsuoka, Y.; Harada, S.; Sultana, S. Use of multi-beam sonar to map seagrass beds in Otsuchi Bay, on the Sanriku Coast of Japan. *Aquat. Living Resour.* **2003**, *16*, 223–230. [CrossRef]
38. Komatsu, T.; Ben Mustapha, K.; Shibata, K.; Hantani, K.; Ohmura, T.; Sammari, C.; Igarashi, C.; El Abed, A. Mapping Posidonia Meadows on Messioua Bank off Zarzis, Tunisia, Using Multi-Beam Sonar and GIS. In *GIS/Spatial Analyses in Fisheries and Aquatic Sciences*; Nishida, T., Kaiola, P.J., Hollingworth, C.E., Eds.; Fishery-Aquatic GIS Research Group: Saitama, Japan, 2004; pp. 83–100.
39. Parnum, I.M.; Gavrilov, A.N. High-frequency multibeam echo-sounder measurements of seafloor backscatter in shallow water: Part 1–Data acquisition and processing. *Underw. Technol.* **2011**, *30*, 3–12. [CrossRef]
40. Tecchiato, S.; Collins, L.; Parnum, I.; Stevens, A. The influence of geomorphology and sedimentary processes on benthic habitat distribution and littoral sediment dynamics: Geraldton, Western Australia. *Mar. Geol.* **2015**, *359*, 148–162. [CrossRef]
41. De Falco, G.; Tonielli, R.; di Martino, G.; Innangi, S.; Simeone, S.; Michael Parnum, I. Relationships between multibeam backscatter, sediment grain size and *Posidonia oceanica* seagrass distribution. *Cont. Shelf Res.* **2010**, *30*, 1941–1950. [CrossRef]
42. Parnum, I.M. Benthic Habitat Mapping Using Multibeam Sonar System. PhD Thesis, Department of Imaging and Applied Physics, Curtin University of Technology, Perth, Australia, 2007; p. 213.
43. Lyons, A.P.; Abraham, D.A. Statistical characterization of high-frequency shallow-water seafloor backscatter. *J. Acoust. Soc. Am.* **1999**, *106*, 1307–1315. [CrossRef]
44. Riegl, B.; Moyer, R.P.; Morris, L.; Virnstein, R.; Dodge, R.E. Determination of the distribution of shallow-water seagrass and drift algae communities with acoustic searfloor discrimination. *Rev. Biol. Trop.* **2005**, *53*, 165–174. [PubMed]
45. Wilson, P.S.; Dunton, K.H. Laboratory investigation of the acoustic response of seagrass tissue in the frequency band 0.5–2.5 kHz. *J. Acoust. Soc. Am.* **2009**, *125*, 1951–1959. [CrossRef] [PubMed]
46. Anderson, J.T.; van Holliday, D.; Kloser, R.; Reid, D.G.; Simard, Y. Acoustic seabed classification: Current practice and future directions. *ICES J. Mar. Sci. J. Cons.* **2008**, *65*, 1004–1011. [CrossRef]
47. Di Maida, G.; Tomasello, A.; Luzzu, F.; Scannavino, A.; Pirrotta, M.; Orestano, C.; Calvo, S. Discriminating between *Posidonia oceanica* meadows and sand substratum using multibeam sonar. *ICES J. Mar. Sci. J. Cons.* **2011**, *68*, 12–19. [CrossRef]
48. Lurton, X. *An Introduction to Underwater Acoustics: Principles and Applications*; Springer: Berlin, Germany, 2002; p. 347.
49. Komatsu, T.; Ohtaki, T.; Sakamoto, S.; Sawayama, S.; Hamana, Y.; Shibata, M.; Shibata, K.; Sasa, S. Impact of the 2011 Tsunami on Seagrass and Seaweed Beds in Otsuchi Bay, Sanriku Coast, Japan. In *Marine Productivity: Perturbations and Resilience of Socio-Ecosystems*; Ceccaldi, H.J., Hénocque, Y., Koike, Y., Komatsu, T., Stora, G., Tusseau-Vuillemin, M.-H., Eds.; Springer International Publishing AG: Cham, Switzerland, 2015; pp. 43–53.
50. Sakamoto, S.X.; Sasa, S.; Sawayama, S.; Tsujimoto, R.; Terauchi, G.; Yagi, H.; Komatsu, T. Impact of huge tsunami in March 2011 on seaweed bed distributions in Shizugawa Bay, Sanriku Coast, revealed by remote sensing. *Proc. SPIE* **2012**. [CrossRef]
51. Sasa, S.; Sawayama, S.; Sakamoto, S.; Tsujimoto, R.; Terauchi, G.; Yagi, H.; Komatsu, T. Did huge tsunami on 11 March 2011 impact seagrass bed distributions in Shizugawa Bay, Sanriku Coast, Japan? *Proc. SPIE* **2012**. [CrossRef]
52. Applanix Corp. POS MV V5 Installation and Operation Guide. Document # PUBS-MAN-004291, Revision: 11, Date: 8-December-2015. Available online: www.applanix.com/products/marine/pos-mv/423-operations-manual-v5-.html (accessed on 22 January 2016).

53. Short, F.T.; McKenzie, L.J.; Coles, R.G.; Vidler, K.P. *Seagrassnet Manual for Scientific Monitoring of Seagrass Habitat*; Queensland Department of Primary Industry, Queensland Fisheries Service: Cairns, Australia, 2002; p. 56.
54. Almar, H. How to Total Propagated Uncertainty. from QPS. Available online: https://confluence.qps.nl/s/-wQfAg (accessed on 21 August 2015).
55. Almar, H. Tips and Tricks. Retrieved 16 September 2015, from QPS. Available online: https://confluence.qps.nl/x/3QwfAg (accessed on 16 September 2015).
56. IHO (International Hydrographic Organization). *IHO Standards for Hydrographic Surveys*; IHO: Monaco, 2008; p. 17.
57. Innangi, S.; Barra, M.; di Martino, G.; Parnum, I.M.; Tonielli, R.; Mazzola, S. Reson SeaBat 8125 backscatter data as a tool for seabed characterization (Central Mediterranean, Southern Italy): Results from different processing approaches. *Appl. Acoust.* **2015**, *87*, 109–122. [CrossRef]

© 2016 by the authors; licensee MDPI, Basel, Switzerland. This article is an open access article distributed under the terms and conditions of the Creative Commons by Attribution (CC-BY) license (http://creativecommons.org/licenses/by/4.0/).